THAPATHALI CAMPUS
Institute of Engineering
Tribhuvan University

Seismic performance evaluation of stone masonry wallet

Paras Khati[a], Hari Ram Parajuli[a,*]

[a]Department of Civil Engineering, Pulchowk Campus, Tribhuvan University, Nepal

ARTICLE INFO

Abstract

This study focuses on the seismic performance evaluation of unreinforced stone masonry wall piers in typical residential buildings in Nepal, utilizing the finite element method (FEM). The seismic coefficient method is employed to calculate the horizontal and vertical loads on the masonry wall pier. Key findings indicate that the wall piers are more vulnerable to shear failure and diagonal tension compared to toe crushing and rocking failures. The failure modes suggest that stone masonry buildings in Nepal typically fail due to shear and tension during earthquakes. From this analysis the shear stress reached 1.67 N/mm^2 at the end of the load steps. Additionally, a simplified micro-analysis reveals the in-depth behavior and local failure mechanisms of the masonry under seismic loads.

1. Introduction

Nepal is situated in one of the most seismically active zones in the world, primarily due to the ongoing collision between the Indian and Tibetan tectonic plates. This tectonic activity has resulted in frequent earthquakes and fault movements across the region [1]. Nepal has experienced numerous significant earthquakes, such as the 1988 Eastern Nepal earthquake M6.8, the 1934 Nepal-Bihar earthquake M8.1, and the 2015 Gorkha earthquake M7.8 [2][3]. Other notable earthquakes in the Himalayan region include the 2005 Kashmir earthquake in Pakistan Mw 7.6, the 1950 Assam earthquake in India (Mw 8.5), the 1505 Nepal earthquake Mw 8.3, the 1897 Shillong earthquake Mw 8.3 [1].

The Gorkha earthquake of April 25, 2015, caused widespread destruction, with nearly 81% of residential buildings damaged or destroyed, most of which were stone masonry structures with mud mortar [4][5]. Approximately one million houses were affected. More recently, the September 2024 Ramidanda, Jajarkot earthquake in western Nepal damaged around 100,000 houses, predominantly low-strength mud-bonded stone masonry buildings [6]. Even moderate shaking in these areas led to significant damage and rendered many homes unusable.

The performance of stone masonry structures during earthquakes is highly dependent on the quality of construction, including the methods used, the quality of materials, and the workmanship involved [7]. Equally important is the structural adequacy of the components, which determines the resilience of these buildings under seismic stress.

Stone masonry buildings are widespread in rural Nepal, primarily because of the abundant availability of materials and their low cost. Most of these buildings are constructed using random rubble masonry, where stones are stacked with or without mud mortar. However, seismic forces are often not considered in their design. As a result, these buildings have several inherent weaknesses, including low strength, heavy mass, high density, and brittleness, which make them particularly vulnerable to earthquake loads dissipating higher energy amount [8].

Masonry buildings are constructed in layers and exhibit poor performance both in-plane and out-of-plane due to issues such as bulging and delamination of the layers. The primary causes of failure are the lack of tensile strength in the masonry units and the weak shear strength of the mortar. These deficiencies, when exposed to lateral seismic loads, lead to both local and global failures.

*Corresponding author:
✉ hariparajuli@ioe.edu.np (H.R. Parajuli)

Therefore, the objective of studying the seismic performance of stone masonry walls and structures is to understand their vulnerability and to develop strategies for improving their resilience.

2. Theoretical background

Stone masonry is a composite material of stone and mud mortar. The stone and mud mortar have a wide range of mechanical and structural performance due to varying of compositions.

2.1. Failure mechanism of masonry

Stone masonry is a composite material consisting of stone and mud mortar, with the mechanical and structural performance of the masonry varying widely due to differences in the composition of both materials [9]. During earthquakes, stone masonry buildings are particularly susceptible due to their heavy walls and roofs, which contribute to significant inertia forces. The main failure mechanisms in masonry piers subjected to seismic loads are [10]:

- **Shear Failure:** This occurs when the principal stresses developed in the wall exceed its tensile strength. It is characterized by diagonal cracks that appear when the masonry fails under lateral in-plane seismic loads.

- **Sliding Failure:** This mode of failure occurs when the masonry slides along its foundation or horizontal joints, typically due to weak horizontal joints and low friction between layers. It happens in cases of low vertical load and poor bonding strength, causing a crack at the interface and subsequent sliding between layers.

2.2. Modeling of masonry

Masonry, composed of stone and mortar, is a complex material, and studying its behavior through physical experiments can be expensive and time-consuming. As a result, numerical analysis becomes a valuable alternative for assessing its performance, particularly in structural engineering. Different numerical approaches are available to model masonry behavior, especially within finite element analysis (FEA). These approaches vary in complexity, depending on the scale of detail required. The three primary modeling strategies for masonry identified in the field are summarized [11][12][13].

1. **Micro-scale model:** This is the most detailed approach, where individual masonry units (stones or bricks) and mortar are modeled as separate entities. The interface between the unit and mortar

is represented using discontinuous elements, allowing cracks to form at the joints [10]. It offers the highest accuracy in capturing the local behavior of masonry, including crack initiation and propagation. In contrast, it requires significant computational resources, making it impractical for large structures or complex simulations. It is best suited for localized studies.

2. **Simplified micro model:** This a less detailed approach where the masonry units are modeled with continuum elements, but the thickness of the mortar joint is simplified, often expanded to half its actual thickness. The interface between the units and mortar is treated as a discontinuous element, simplifying the interactions. It balances accuracy and computational efficiency, capturing some localized behaviors while reducing the complexity of the model. But it still requires moderate computational resources and may not capture fine details of failure mechanisms.

3. **Macro-scale model:** This is the most simplified approach, where the masonry structure is treated as a homogenized continuum, ignoring the individual units and mortar. The entire structure is modeled as either isotropic or anisotropic. It has highly computationally efficient and practical for large-scale analysis of entire structures. It is widely used in engineering applications where detailed local behavior is less critical. But it lacks the precision of micro-scale models, as it does not account for specific interactions between units and mortar or localized failure mechanisms.

These modeling techniques [14] help engineers and researchers assess the seismic performance, failure mechanisms, and overall behavior of masonry structures under various conditions without the need for extensive experimental testing.

3. Methodology

A detailed procedure was adopted for the modeling of the masonry wall. A simple masonry wall was selected for this study. An isotropic homogeneous model was chosen, using the concrete damaged plasticity model to represent the behavior of the material. The horizontal and vertical loads applied to the model were calculated manually using the seismic coefficient method and then applied to the model for analysis [15][16].

3.1. Model

To investigate the behavior of masonry, a stone masonry wallet was prepared. The masonry wall with the dimensions, length: 1500 mm, width: 350 mm, height: 1800

mm as shown in the Figure 1 was modelled. The vertical and horizontal loads were calculated using the seismic coefficient method [15][16] and applied to the RC beam of the masonry wall. The model assumes a strong floor in contact with the ground to replicate realistic conditions. The horizontal reaction was calculated at the base of the wall, while the top displacement was measured at the top of the masonry wall.
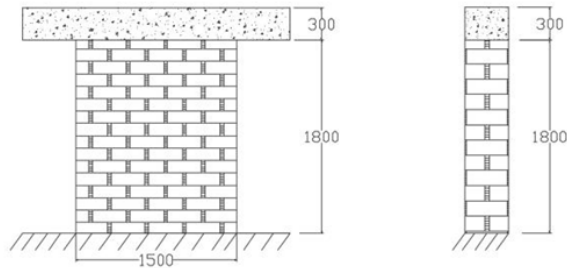

Figure 1: Geometry of wall front and side view

The Finite Element Method (FEM), was used to evaluate the seismic performance of stone masonry walls. divides the modeling process into several key modules, guiding the user through the various stages of analysis [17][18]. The C3D8R (ABAQUS 2012) element (Figure 2), a linear brick element with reduced integration, was selected for the representation of wall elements. This element has 8 nodes and is commonly used for solid structures like masonry walls. The reduced integration feature helps prevent shear locking and improves computational efficiency, making it ideal for analyzing stone masonry structures. The designation "C3D8R" is explained as C: Continuum element, 3D: 3-dimensional, 8: 8-noded element, R: Reduced integration.
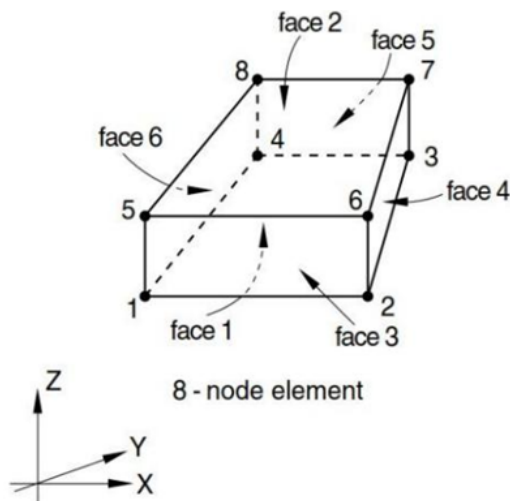

Figure 2: C3D8R for solids

This element is widely used to model masonry which re-

quires simpler setups and quicker calculation as shown in Figure 2. The linear interpolation used in each direction makes the C3D8R element efficient for first-order models.

3.2. Model setup and loading

The wall model (Figure 3) has three constituents; concrete beam, full stone wall, and foundation plate. The model was then assembled and meshed to the desired resolution. In the property module, material properties such as density and elasticity were defined for each part. For the masonry part, the concrete damaged plasticity model was applied to simulate the behavior under seismic loads.
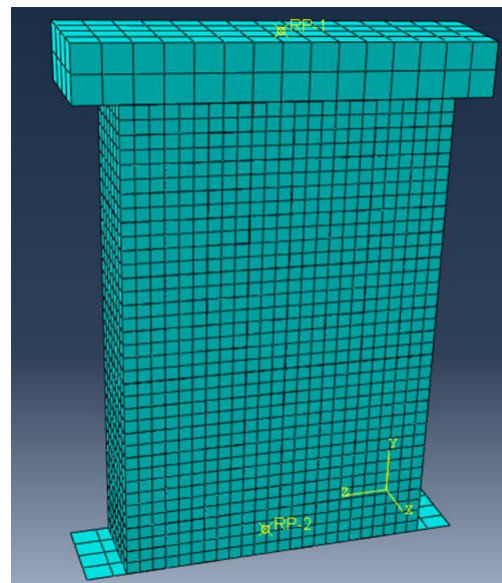

Figure 3: Assembly of meshed model

3.2.1. Elastic properties

The elastic properties of concrete (M20 grade) are mentioned in the Table 1.

Table 1: Elastic properties of concrete and masonry

Properties	Concrete	Masonry
Density (kg/m^3)	2500	200
Modulus of Elasticity (MPa)	22360	15500
Poisson Ratio	0.15	0.2

3.2.2. Inelastic properties

The yield stress of concrete is calculated as the permissible stress multiplied by the factor of safety (FOS) and given in Table 2.

Table 2: Yield stress (MPa) of concrete

Mode	Permissible	FOS	Yield
Bending	7	3	21
Compression	5	4	21

Table 3: Plasticity parameters

Dilation Angle (ψ)	Eccentricity	f_{bo}/f_{co}	K_c	μ
37	0.1	1.16	0.667	0

3.2.3. Plastic parameters

Drucker-Prager (Figure 4) model is used to calculate the non-linearity and crack opening model for masonry. The required parameter (Table 3) are as follows.
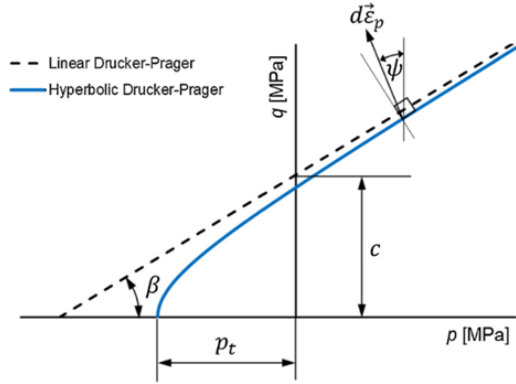

Figure 4: Drucker-Prager yield criteria

Dilation angle, $\psi = 37°$, is taken in the p-q plane as per the Drucker-Prager yield criterion. Eccentricity is taken as 0.1, which defines the rate at which the hyperbolic flow potential approaches its asymptote. The ratio $\frac{f_{bo}}{f_{co}}$, representing the equivalent biaxial compressive yield stress to the initial uniaxial compressive yield stress, is taken as 1.16. The parameter K_c must satisfy the yield condition, and thus $0.5 < K_c < 1$ is taken as $\frac{2}{3}$. The viscosity parameter (μ), used for the viscoplastic regularization in the constitutive equation, is considered to be zero.
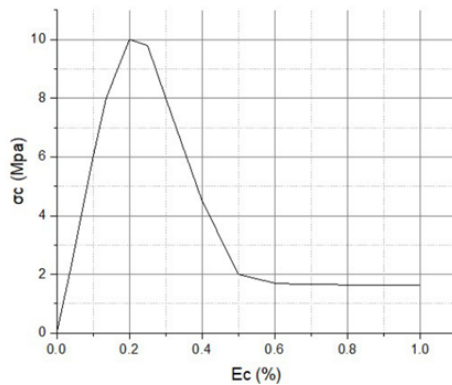

Figure 5: Stress strain curve in compression

3.2.4. Compressive behavior

Compressive behavior beyond the elastic range is defined using a tabular function of stress over the inelastic curve as shown in the Figure 5 which automatically calculates plastic strains from already known inelastic strains.

The elastic strain in compression is given by:

$$\epsilon_{co}^{el} = \frac{\sigma_c}{E_0} \quad (1)$$

The inelastic strain in compression is given by:

$$\epsilon_c^{in} = \epsilon_c - \epsilon_{co}^{el} \quad (2)$$

The plastic strain is calculated by:

$$\epsilon_c^{pl} = \epsilon_c^{in} - \frac{d_c}{1 - d_c} \cdot \frac{\sigma_c}{E_0} \quad (3)$$

Here, d_c is the damage parameter, which is obtained from:

$$d_c = \frac{\sigma_c}{\sigma_c^I} \quad (4)$$

The resulting inelastic strains and damage parameters corresponding to yield stresses are tabulated in Table 4.

Table 4: Inelastic parameters (compressive)

ϵ_c	σ_c	d_c	ϵ_{co}^{el}	ϵ_c^{in}	ϵ_c^{pl}
0.000	0.000	0.000	0.0000	0.000	0.000
0.035	2.000	0.200	0.0003	0.035	0.034
0.100	6.000	0.200	0.0010	0.099	0.099
0.136	8.000	0.200	0.0013	0.135	0.134
0.200	10.000	0.200	0.0017	0.198	0.198
0.250	9.800	0.200	0.0016	0.248	0.248
0.300	8.000	0.200	0.0013	0.299	0.298
0.400	4.500	0.550	0.0008	0.399	0.398
0.500	2.000	0.800	0.0003	0.499	0.498
0.600	1.700	0.836	0.0003	0.599	0.598
0.700	1.650	0.835	0.0003	0.699	0.698
1.000	1.645	0.836	0.0003	0.999	0.998

Similarly, the damage parameter, elastic strain, inelastic

strain and plastic strain for the tensile behavior can be generated using the tensile curve.

The elastic strain in tension is given by:

$$\epsilon_{to}^{el} = \frac{\sigma_t}{E_0} \tag{5}$$

The inelastic strain in tension is given by:

$$\epsilon_t^{in} = \epsilon_t - \epsilon_{to}^{el} \tag{6}$$

The plastic strain is calculated by:

$$\epsilon_t^{pl} = \epsilon_t^{in} - \frac{d_t}{1 - d_t} \cdot \frac{\sigma_t}{E_0} \tag{7}$$

Here, d_t is the damage parameter, which is obtained from:

$$d_t = \frac{\sigma_t}{\sigma_t^I} \tag{8}$$

Where σ_t^I is the tensile strength of the masonry. The resulting inelastic strains and damage parameters corresponding to yield stresses are tabulated in Table 5.

Table 5: Inelastic parameters (tensile)

ϵ_t	σ_t	d_t	ϵ_{to}^{el}	ϵ_t^{in}	ϵ_t^{pl}
0.000	0.00	0.000	0.0000	0.0000	0.0000
0.005	0.70	0.000	0.0001	0.0499	0.0499
0.100	1.37	0.000	0.0002	0.0998	0.0998
0.110	1.40	0.000	0.0002	0.1098	0.1098
0.150	0.48	0.952	0.0001	0.1499	0.1483
0.200	0.20	0.980	0.0000	0.2000	0.1983
0.250	0.10	0.990	0.0000	0.2500	0.2483
0.300	0.05	0.995	0.0000	0.3000	0.2983
0.340	0.03	0.997	0.0000	0.3400	0.3383

4. Result and discussion

The module is executed and analyzed. After assembling the different parts into the required masonry wall type, the model is meshed, and the loading is applied to the wall. Steps for the analysis are defined, and the history output is specified. Once the analysis begins to run, the model can be visualized using the visualization module for each increment of the step time. Upon completion of the job, X-Y plots can be extracted from the history output, and the stress, strain, and damage conditions can be visualized for each time step.

4.1. Force displacement curve

The reaction force at the base is plotted with the displacement at the top of the wall. A non-linear force deformation curve is found. The Force-Displacement curve from the result is shown in Figure 6.
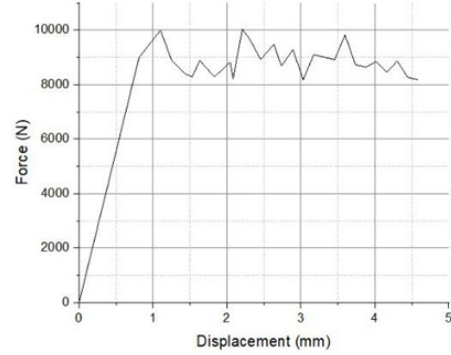

Figure 6: Force displacement relation

4.2. Stress-strain visualization

The stress-strain contours of the output results are presented, highlighting the concentration of von-Mises stresses at various performance levels. The contours show compression at the top and bottom edges of the wall, occurring at alternating corners. Additionally, a reduction in stress is observed along the diagonal, which is attributed to tension damage (Figure 7 and 8). As the analysis progresses through each time step, an increase in stress concentration is noted at the toe of the wall pier
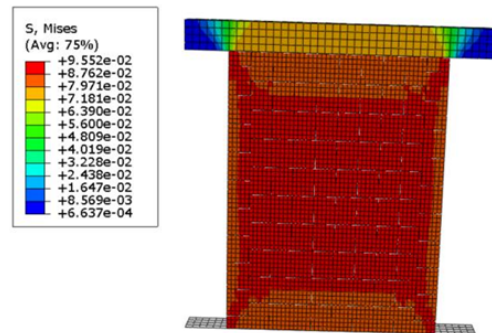

Figure 7: Initial stresses developed in wall

4.3. Damage visualization

This section presents the progression of damage at each performance level, which can be clearly observed. Since masonry is inherently weak in tension, the model provides a satisfactory visualization of tension damage (Figure 9 and 10). The damage initiation begins at one corner of the wall, where tension is generated due to flexure.
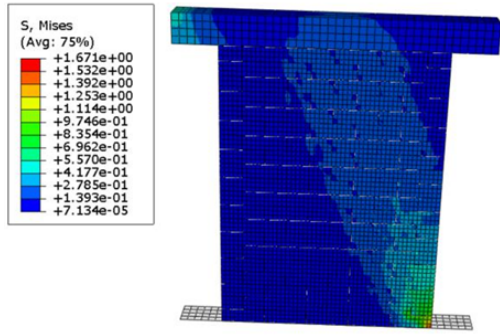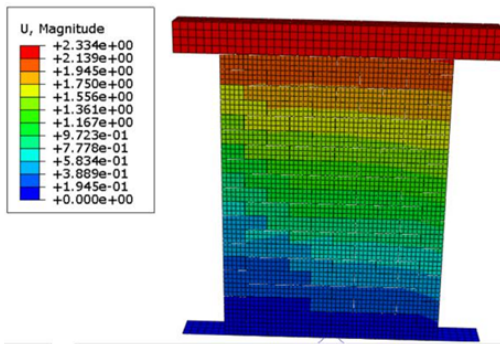
Figure 8: Final Von-Mieses Stress
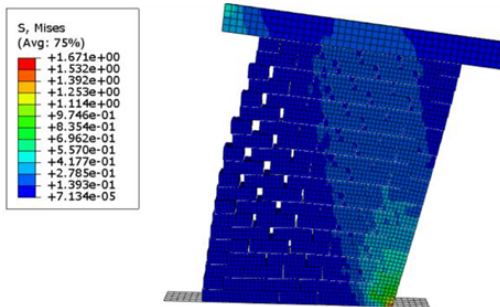

Figure 9: Final displacement on wall

Figure 10: Final damage observed in wall

5. Conclusion

In this study, numerical analysis was performed on a masonry wall pier, focusing on typical residential unreinforced stone masonry buildings. The goal is to evaluate the seismic performance of these buildings and explore ways to improve their resistance to future earthquakes. The study revealed that the existing building forms are highly vulnerable to seismic activity.

A two-dimensional masonry wall model was developed, representing a pier from a stone masonry building. To account for the influence of the mortar, interface elements were incorporated, and contact between the stone elements was defined. The model simulated the time-dependent sliding and separation of the stone elements along these interfaces. The simplified micro-analysis captured the behavior of the masonry, showing detailed local failure mechanisms within the wall element. The key findings are following:

1. Shear failure mode was observed in the masonry pier, rather than the rocking failure mode. Rocking failure generally occurs when a single block is subjected to large vertical and shear loads simultaneously (due to moments). The simplified micro-modeling showed that the masonry wall fails in shear and tension before experiencing rocking failure.

2. The shear stresses developed in the masonry wall reached 1.67 N/mm^2 at the 100th step of the analysis, exceeding the permissible stress of 0.153 N/mm^2, leading to shear failure.

3. The displacement contour indicated maximum displacement at the top of the wall, measured at 2.33 mm, which decreased to zero at the base of the wall, as it was fixed.

4. Stress concentration was highest at the toe of the wall, increasing progressively from 0.535 N/mm^2 at step 1 to 1.671 N/mm^2 at step 100. The reduction in stress along the diagonal was due to tension damage, which developed further with each time step.

5. The results of the analysis align with the experimental verification conducted by Lemos (2019), which confirmed that shear failure is more likely in masonry piers than rocking failure.

6. The Finite Element Analysis (FEA) assumed the material to be isotropic, whereas in reality, masonry walls are a composite of masonry units and mortar (anisotropic). Despite this simplification, the results showed good agreement with field data.

7. The study acknowledges that further detailed experimental work is needed, as many material properties were assumed based on empirical formulas. There is limited literature available on the performance of stone masonry walls, and more experimental research could help validate and refine the findings.

References

[1] Bilham R. Himalayan earthquakes: A review of historical seismicity and early 21st century slip potential[J/OL]. Geological Society Special Publication, 2019, 483: 423-482. DOI: 10.1144/SP483.16.

[2] Panta M. A step towards a historical seismicity of nepal[J]. Adarsa, 2002, 2: 30-35.

[3] Rana B. Great nepal earthquake 1934[M]. Third ed. Sahayogi Press, Tripureshwor (in Nepali), 1935.

[4] GoN. Nepal earthquake 2015—post disaster needs assessment: B: Sector Reports[M]. 2015.

[5] Gautam D, Chaulagain H. Structural performance and associated lessons to be learned from world earthquakes in nepal after 25 april 2015 (mw 7.8) gorkha earthquake[J]. Engineering Failure Analysis, 2016, 68: 222-243.

[6] NDRRMA. Nepal earthquake response, situation reports[M]. 2023.

[7] Chalise B, Suwal R. Seismic performance of masonry buildings during the recent gorkha earthquake in nepal[C]// International Conference on Innovation in Structural Engineering (IC ISE). 2015.

[8] Shakya K, Pant D, Maharjan M, et al. Lessons learned from the performance of buildings during the september 18, 2011 earthquake in nepal[J]. 2013.

[9] Javed M. Seismic risk assessment of unreinforced brick masonry buildings system of northern pakistan[D]. Civil Engineering Department, 2009.

[10] Lourenço P, De Borst R, Rots J. A plane stress softening plasticity model for orthotropic materials[J]. International Journal for Numerical Methods in Engineering, 1997, 40(21): 4033-4057.

[11] Tzamtzis A, Nath B. Application of three-dimensional interface element to non-linear static and dynamic finite element analysis of discontinuous systems[C]// Engineering System Design and Analysis, ASME: PD-Vol. 47-1. 1992: 1.

[12] Tzamtzis A, Asteris P. A 3d model for non-linear microscopic fe analysis of masonry structures[C]// Proceedings of the Sixth International Masonry Conference. London, 2002: 493-497.

[13] Tzamtzis A, Asteris P. Fe analysis of complex discontinuous and jointed structural systems[J]. Electronic Journal of Structural Engineering, 2004, 1.

[14] Parajuli H, Ghimire A. Investigation on lateral loading on masonry walls[J]. Nepal Journal of Science and Technology (NJST), 2021.

[15] IS. Criteria for earthquake-resistant design of structures[M]. Bureau of Indian Standards, New Delhi, 2002: 1-24.

[16] Maskey P, Tamrakar M, Bista M, et al. Nbc105: 2019 seismic design of buildings in nepal: New provisions in the code[M]. 2020.

[17] Teomete E, Aktas E. Structural analyses and assessment of the historical kamanlı mosque in izmir, turkey[J]. Journal of Performance of Constructed Facilities, 2010, 24(4): 353-364.

[18] Rafiq A, Fahad M. Computational modelling of unconfined/unreinforced masonry wall[D]. University of Engineering and Technology, Peshawar, Pakistan, 2016.

[19] Chidiac S, Foo S, Cheung M. Seismic guidelines for stone-masonry components and structures[C]// Proceedings of the International Conference on the Seismic Performance of Traditional Buildings. Turkey, 2000.

[20] Lourenço P. Computational strategy for masonry structures[D]. Delft University of Technology and DIANA Research, 1996.

[21] Scripting user's manual: 6.11[M/OL]. 2012. http://130.149,89(2080/.